A straightforward approach to high purity sodium silicide Na4Si4

Yang Song, Isabel Gómez-Recio, Ram Kumar, Cristina Coelho Diogo, Sandra Casale, Isabelle Génois, David Portehault

A straightforward approach to high purity sodium silicide Na_4Si_4

Yang Song,[a] Isabel Gómez-Recio,[a] Ram Kumar,[a] Cristina Coelho Diogo,[b] Sandra Casale,[c] Isabelle Génois[a] and David Portehault*[a]

Sodium silicide Na_4Si_4 is a reductive and reactive source of silicon highly relevant to designing non-oxidic silicon materials, including clathrates, various silicon allotropes, and metal silicides. Despite the impor-tance of this compound, its production in high amounts and high purity is still a bottleneck with reported methods. In this work, we demonstrate that readily available silicon nanoparticles react with sodium hydride with a stoichiometry close to the theoretical one and at a temperature of 395 °C for shorter duration than previously reported. This enhanced reactivity of silicon nanoparticles makes the procedure robust and less dependent on experimental parameters, such as gas flow. As a result, we deliver a pro-cedure to achieve Na_4Si_4 with purity of ca. 98 mol% at the gram scale. We show that this compound is an efficient precursor to deliver selectively type I and type II sodium silicon clathrates depending on the con-ditions of thermal decomposition.

a Sorbonne Université, CNRS, Collège de France, Laboratoire de Chimie de la Matière Condensée de Paris (CMCP), 4 place Jussieu, F-75005 Paris,Condensée de Paris (CMCP), 4 place Jussieu, F-75005 Paris, France. France.

b Sorbonne Université, CNRS, Institut des Matériaux de Paris-Centre, IMPC, 4 place Jussieu, F-75005 Paris, France.

c Sorbonne Université, CNRS, Laboratoire de Réactivité de Surface (LRS), 4 place Jussieu, F-75005 Paris, France.

E-mail: david.portehault@sorbonne-universite.fr

Silicon-based materials are involved in many domains from electronic devices, to catalysts, to biomedical technology.[1–5] Research efforts towards novel forms of silicon and silicon-based materials have yielded – among others – silicon clathrates,[6,7] a variety of new silicon allotropes,[8–10] and transition metal silicides.[5,11,12] Silicon-based nanomaterials also provide an additional dimension to the phase space, in order to adjust properties with *e.g.* silicon nanoparticles,[13,14] nanoporous and mesostructured frameworks,[15] as well as metal silicide nanocrystals.[5,11] These materials can be produced by planar deposition methods that use gas-phase silicon-containing molecules,[13,16,17] or by solid-state reactions employing elemental silicon or alkali silicides.[7,8] These reactions can also be mediated in liquid phase.[6,11,14,18] Herein we focus on a specific silicon source: sodium silicide Na_4Si_4.[19–21]

Na_4Si_4 is a Zintl phase that contains tetrahedral polyanions $[Si_4]^{4-}$, which are isoelectronic and then isostructural to the P_4 molecule. They are compensated by Na^+ cations as a result of charge transfer from electropositive sodium to silicon. The $[Si_4]^{4-}$ clusters are highly reactive, which has been discussed to provide a potential portable hydrogen source upon reaction with water.[22] Additionally, the low oxidation state of silicon and the fact that Si is only involved in intra-cluster bonds provide high flexibility for designing silicon-based materials under mild conditions. For instance, depending on the conditions of decomposition, Na_4Si_4 yields readily silicon clathrates[6,7] or silicon nanoparticles.[14]

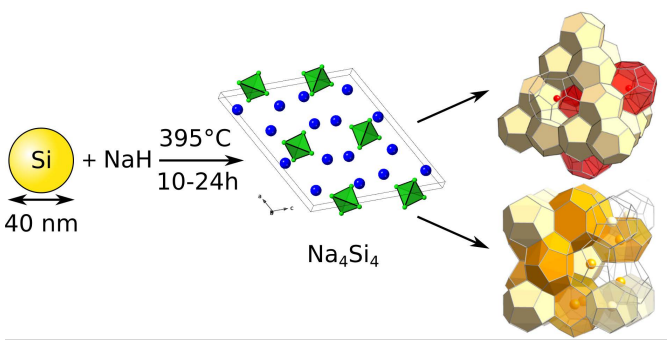

Unfortunately, Na_4Si_4 is usually accompanied by elemental silicon and sodium impurities,[6,7,19,23–27] which are detrimental to the precise control of the reactions where sodium silicide is used afterward. For instance, Si impurities are relatively inert and remain in the final product. Na impurities can also act as additional reducing agent,[11] although they might be separated from Na_4Si_4 by vacuum heating at 230–300 °C.[19,23,25] Hence, a synthesis procedure for high purity Na_4Si_4 (*ca.* 90 mol%) is yet to be developed.

The reaction between elemental sodium and silicon is the most known approach to obtain Na_4Si_4 (Table S1).[23,25] To avoid sodium evaporation, the reagents must be sealed by arc-welding in tantalum or niobium tubes, further introduced into silica ampules or steel pressure vessels and heated at 650–750 °C for several days to one week. The procedure requires specific equipment and metal containers not readily available in most laboratories. It also requires special care to avoid the presence of sodium at the welded closure, which is detrimental to sealing and reproducibility.[24] Overall, the resulting material encompasses Na_4Si_4 and excess elemental silicon and/or sodium. For instance, a stoichiometric mixture

of silicon and sodium yields a mixture of Si and Na_4Si_4 with a purity of *ca.* 44 mol% (Table S1).[6] Another approach involves the reaction of sodium with silica gel to yield *ca.* 15 mol% Na_4Si_4 mixed with Na_2SiO_3 (Table S1).[28,29] A third method was first reported by Ma *et al.*[24] and enabled a decrease by few hundreds of degrees of the synthesis temperature, by triggering the reaction between previously ball-milled sodium hydride and silicon powders at 420 °C under argon flow over several days. The procedure did not require any specific container nor sealing and then appeared simple, but a long ball-milling pretreatment of 0.5–1 h was required.[19,30] More importantly, the outcome strongly depended on experimental parameters, including the preliminary ball-milling time and especially the argon flow rate, since reaction intermediates (sodium) and by-products (dihydrogen) are volatile or gaseous at the reaction temperature. Therefore, despite the attractiveness of this procedure, reaching high purity (*ca.* 90 mol%) sodium silicide remains an arduous task: a large excess of sodium hydride is required, while elemental silicon and sodium are commonly encountered as impurities.

Herein we report a procedure to enhance the reactivity of silicon with sodium hydride by using silicon nanoparticles as reagents and by carefully controlling experimental parameters (Fig. 1). Thanks to this approach, we demonstrate the ability with regular lab equipment to reproducibly produce sodium silicide with a purity of *ca.* 98 mol% and at the scale of several hundreds of milligrams, both features strongly exceeding those previously reported.[24] We then deliver a simple scalable protocol that will enable wide-spread use of this material.

Experimental methods

Commercial NaH (95%, Sigma-Aldrich) and bulk Si powder (99%, Sigma-Aldrich) were used as received. Commercially available silicon nanoparticles (99%) were obtained from Nanomakers© (Fig. S1 and S2), France. All the reagents and products were stored and manipulated in an argon-filled glovebox free of H_2O (<0.5 ppm) and O_2 (<0.5 ppm) and with standard Schlenk procedures. **Caution:** the Na_4Si_4 powders produced by the procedure described herein are air sensitive and burn spontaneously when exposed to water. All manipulations described were performed by handling these powders under inert atmosphere, except when stated otherwise.

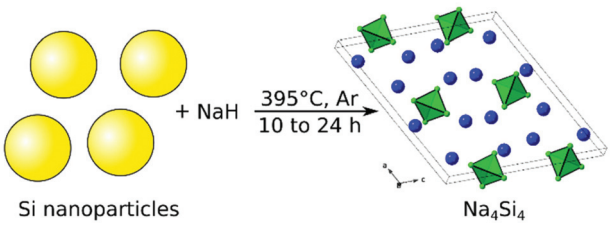

Fig. 1 Scheme of the synthesis route towards high purity Na_4Si_4.

Na_4Si_4 synthesis from Si nanoparticles: 470 mg of NaH (20 mmol) and 500 mg of Si nanoparticles (20 mmol) were firstly ball-milled for 2 minutes at 20 Hz (Retsch MM400 ball mill airtight stainless-steel vial of 50 mL, one steel ball of 62.3 g with a diameter of 23 mm). Then, the fine powder was loaded in a pyrolytic *h*-BN crucible (cylinder ∅ 25 × H60 mm) covered with a cap of pyrolytic *h*-BN, then placed in a bottom closed quartz tube. The tube was heated in a vertical furnace at 395 °C with different reaction times from 2 to 24 hours, under argon flow. The as-synthesized sample was made of a dark pellet with another white pellet on the top. The latter corresponds to Na_2O and NaOH coming from the reaction between NaH and the native silicon oxide layer on the surface of Si nanoparticles (Fig. S2). The upper white pellet was scratched away. The synthesis of Na_4Si_4 under the optimal conditions described in the Results and discussion section was repeated 20 times to ensure reproducibility.

Na_4Si_4 synthesis from bulk Si powder was prepared following the same procedure and reagents proportion described above, but bulk Si powder was used instead of Si nanoparticles. The thermal treatment was performed at 395 °C for 10 hours.

Si clathrates synthesis: The Na_4Si_4 powder (4 mmol) synthesized as described above was loaded in a pyrolytic *h*-BN crucible (∅ 25 × H60 mm) previously dried at 400 °C under vacuum (10^{-3} mbar) for 10 hours to remove adsorbed moisture. The crucible was placed in a bottom-closed quartz tube. The tube was heated in a vertical furnace. Na_8Si_{46} (type I) and Na_xSi_{136} (type II) were obtained by heat treatment at 470 °C and 440 °C, respectively, under dynamic vacuum (10^{-3} mbar) for 90 min. These temperatures were chosen according to the literature.[7] For Na_8Si_{46} (type I), the *h*-BN crucible was covered with an *h*-BN cap prior heating, to maintain a higher Na vapor pressure. For Na_xSi_{136} (type II), the crucible was maintained opened. During the reaction, a thin deposit of Na appeared on the upside cold part of the quartz tube. After dwelling and cooling down, the quartz tube with the *h*-BN crucible and its containment was transferred into an argon-filled glovebox without exposure to air.

Powder X-ray diffraction (XRD) was performed on a Bruker D8 Advance diffractometer equipped with an X-ray source working with Cu Kα radiation. Due to the air-sensitivity of Na_4Si_4, the powder was loaded in an airtight sample holder into an argon-filled glovebox and capped with a protective plastic dome. Beam scattering by the dome gives rise to a broad bump between 15–25° (2θ Cu Kα) (Fig. S3). Powder XRD patterns used for Le Bail analysis were acquired with a step size of 0.029° and an acquisition time of 10 s per step, which correspond to 13 h of measurement. Over this long dur-ation, the sample holder shows evidences of air leaks (see Results and discussion). Otherwise, 5 min fast acquisitions with a step size of 0.050° and an acquisition time of 0.19 s per step were performed as standard program to avoid sample degradation during XRD measurement. Na_4Si_4, Na, Si (diamond structure, *d*-Si) and NaOH were identified according to the ICDD database and the reference cards 04-015-9208, 00-022-0948, 00-027-1402 and 00-035-1009, respectively.

^{29}Si and ^{23}Na magic angle spinning solid-state nuclear magnetic resonance (MAS solid-state NMR) spectra were acquired on a 700 MHz AVANCE III Bruker spectrometer operating at 139.05 MHz and at 185.20 MHz respectively and using a 3.2 mm Bruker triple resonance probe. Samples were transferred to ZrO_2 rotors spun at a MAS rate of 10 kHz for ^{29}Si and 20 kHz for ^{23}Na. A single-pulse excitation was used with a recycle delay of 500s and 400 scans for ^{29}Si and 1 s and 1960 scans for ^{23}Na. ^{29}Si and ^{23}Na chemical shifts were referenced to TMS and 0.1 M NaCl (aq) respectively. The spectra were treated with the DMFIT program.[31]

Energy-dispersive X-ray spectroscopy (EDS) (Oxford Instruments – X-max) on the scanning electron microscope (SEM) was performed on a SEM HITACHI S3400N at 20 kV to determine the composition of the Na_4Si_4 sample. Carbon deposition was required to enable the EDS analysis on insulating sample. In order to avoid equipment damage and for safety concern, air-sensitive Na_4Si_4 samples were pre-neutralized by exposure to air during 4 days.

Transmission electron microscope (TEM) and high resolution TEM (HRTEM) was performed with JEOL JEM 2100 FEG microscope operating at 200 kV. For sample preparation, the powders were dispersed in ethanol. The suspensions were drop casted onto carbon coated copper grids.

Results and discussion

Optimal synthesis of Na_4Si_4

Reaction (1) described below between NaH and Si nanoparticles (1.1 : 1 mol ratio) was performed for 24 hours at 395 °C with an argon flow of 55 mL min^{-1}:

$$4NaH_{(s)} + 4Si_{(s)} \xrightarrow{\Delta} Na_4Si_{4(s)} + 2H_{2(g)} \quad (1)$$

A slight excess of NaH was used in order to account for reaction (2) below, which accounts for the reactivity between sodium hydride and the native oxide layer of silicon particles (simplified as SiO_2):

$$10NaH_{(s)} + 4SiO_{2(s)} \xrightarrow{\Delta} Na_4Si_{4(s)} + 3Na_2O_{(s)} + 5H_2O_{(g)} \quad (2)$$

Under these optimal conditions, Na_4Si_4 with optimized purity was obtained. The atomic ratio between Na and Si was evaluated to Na : Si = 1 : 1.02 by EDS analysis. The formation of Na_4Si_4 (S.G. *C*2/*c*) was supported by Le Bail analysis of the powder XRD pattern (Fig. 2 and Table S2). NaOH was also detected (Fig. 2) and ascribed to leakage of air into the XRD sample holder during the long acquisition of the XRD diagram. This is confirmed by the fact that no crystalline NaOH was observed in a prior fast acquisition on a fresh sample (Fig. S3).

The ^{29}Si MAS solid-state NMR spectrum of Na_4Si_4 (Fig. 3a) shows two resonances centered at −362 and −366 ppm corresponding respectively to the two crystallographic non-equivalent Si sites in the crystal structure.[23] This upfield shift compared to silicon is due to electron transfer from Na to Si.[25]

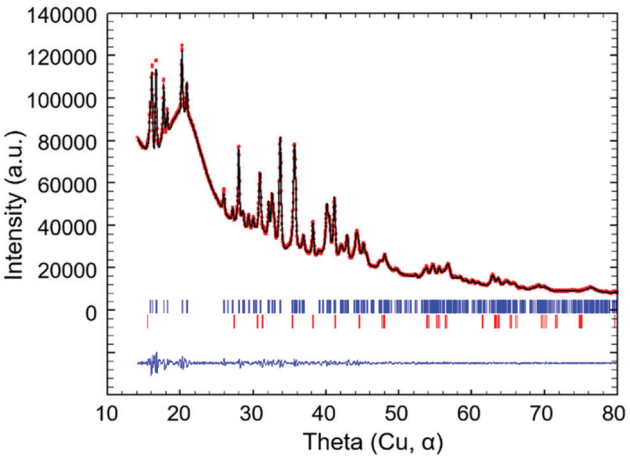

Fig. 2 Le Bail analysis of the XRD pattern of the powder obtained after 24 h at 395 °C under 55 mL min^{-1} Ar flow. The observed pattern, calculated pattern and difference curve are shown in red dots, black curve and blue curve, respectively. Upper blue and lower red tick marks correspond to Na_4Si_4 and NaOH, respectively.

Besides, neither broad signal of amorphous SiO_2 and Si centered at *ca.* −110 and −40 ppm[32,33] nor any contri-bution of *d*-Si expected at *ca.* −80 ppm[34] were observed. It thus confirms the high purity of Na_4Si_4. The ^{23}Na spectrum (Fig. 3b) shows two quadrupolar resonance patterns at 56.3 ppm (C_Q = 1.32 MHz, η_Q = 0.47) and 49.8 ppm (C_Q = 2.34 MHz, η_Q = 0.27) corresponding to two Na crystallographic sites in Na_4Si_4. In addition, no peak at *ca.* 50 ppm corres-ponding to Na_2O could be detected,[35] suggesting no contami-nation from the upper white pellet made mainly of Na_2O and of a minor portion of NaOH (Fig. S4). The thin peak at 18.5 ppm is assigned to crystalline NaOH accounting for less than 5% of the total amount of sodium.[36] As mentioned above, crystalline NaOH could not be detected by XRD in fast acquisition mode (Fig. S3). Its observation by NMR is then ascribed to the degradation of Na_4Si_4 during preparation of NMR analyses.

Overall, EDS, XRD and NMR support the formation of crystalline Na_4Si_4. EDS yields a purity of *ca.* 98 mol%, and amorphous Si is the main impurity. The synthesis yield is about 80%, which corresponds to *ca.* 700 mg of powders, *i.e.* a 10 fold increase compared to previous approaches using the reaction between sodium hydride and silicon (Table S1. This result is achieved with only a slight excess of sodium hydride reagent (10 mol%) compared to previous reports (60–90 mol% excess) (Table S1),[19,30] which enables bypassing purification steps (Table S1). The preliminary ball-milling time is also shortened from over 30 min to only 2 min and the reaction time is further reduced to 24 h. A comparison with the most commonly used reaction between elemental sodium and silicon occurring above 650 °C (Table S1) shows that the reaction time and the temperature are strongly reduced with the approach we describe herein, while purification steps and complex set-ups encompassing metal containers are avoided.

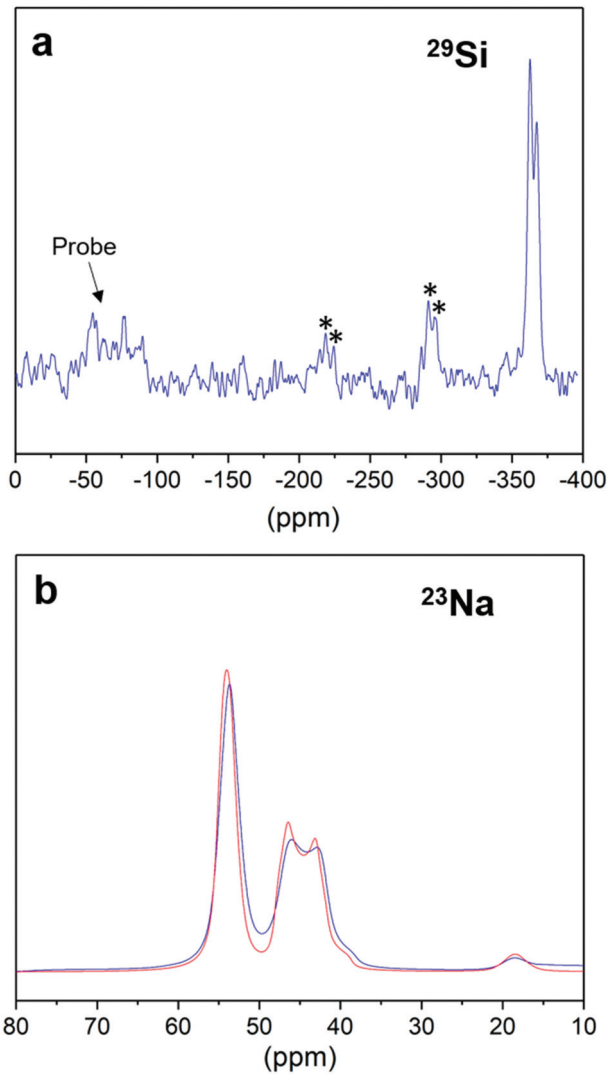

Fig. 3 (a) ^{29}Si and (b) ^{23}Na solid-state NMR spectra of the Na_4Si_4 powder obtained after 24 h at 395 °C under 55 mL min^{-1} Ar flow. Asterisks indicate spinning sidebands. The measured spectra are shown by the blue curves, and the fitting curve is shown in red.

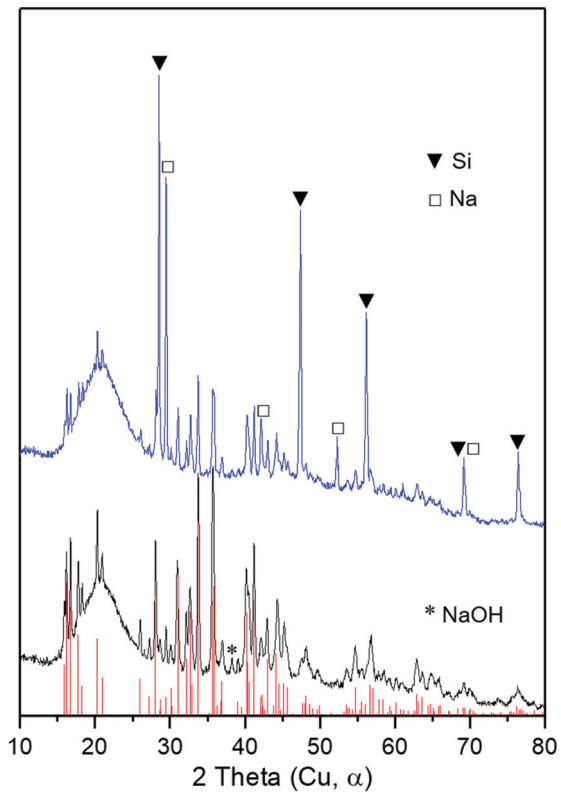

Fig. 4 Powder XRD patterns of the Na_4Si_4 samples synthesized respectively with Si nanoparticles (black bottom curve) and bulk Si powder (blue top curve) at 395 °C for 10 hours with an Ar flow rate 15 mL min^{-1}. Red lines indicate Na_4Si_4 reference. Si, Na, and NaOH impurities are marked on the most informative peaks.

Impact of the Si source

To assess the role of the silicon source in the synthesis, we have followed the same protocol as above but by using bulk Si powder as precursor. The reaction was performed over 10 h under a 15 mL min^{-1} Ar flow rate. The initial NaH : Si ratio was kept at 1.1 : 1 mol. The resulting product was pale grey aggregates. According to XRD (Fig. 4), the main crystalline phases are unreacted Na and Si. Therefore, silicon nanoparticles play a primary role in the completion of the reaction at low temperature and short time. Their higher reactivity ensures a reaction in close-to-stoichiometry reagents ratio compared to bulk Si that required a large excess of NaH (NaH : Si = 1.9 : 1 mol.) to yield Na_4Si_4 as major product.[24,37] Note also that while bulk Si required ball-milling over 1 hour,[19,24] using Si nanoparticles enables shortening the milling step down to 2 min. Likewise, the reaction was performed over 10 to 24 h compared to more than two days as reported for bulk silicon.[24]

Impact of the reaction time

By using Si nanoparticles, we varied the reaction time from 2 to 24 hours to investigate the course of the reaction. XRD (Fig. 5) shows that a 2 h reaction produces crystalline Na_4Si_4 together with Na and Si, as minor phases. The absence of peaks assigned to Na_2O confirmed the thorough separation of Na_4Si_4 from oxidic side-products. NaOH observed is again attributed to air leaks of the XRD sample holder over XRD pattern acquisition. Increasing the reaction time to 10 h decreases the relative intensity of Na and Si peaks. Further decrease of these peaks occurs from 10 to 24 h. It confirms that Si nanoparticles allow shortening the reaction time to 24 h. Note that the XRD pattern obtained at 10 hours is similar to the one previously reported for Na_4Si_4 produced from bulk silicon over 2 days.[24]

Comparison of the results from bulk Si and Si nanoparticles shows a dramatic reduction of reaction time that we ascribe to the reactivity of Si nanoparticles, in relation to their larger interface between NaH and Si, and shorter atomic diffusion paths.

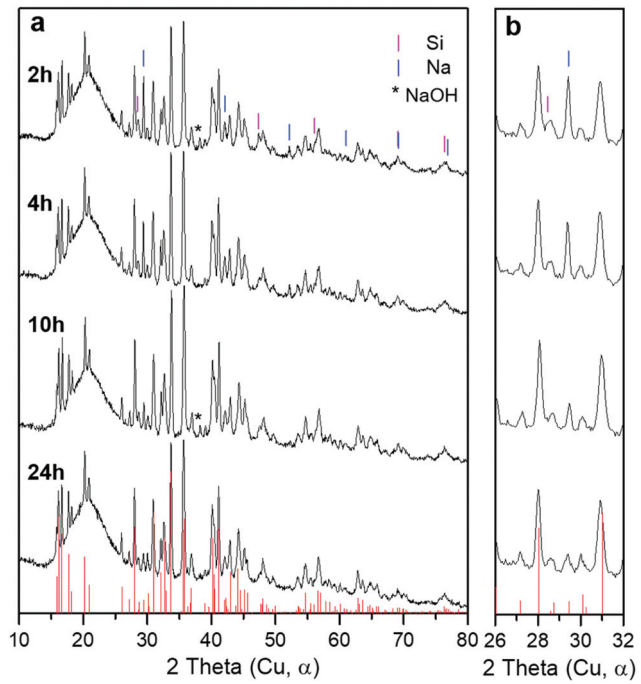

Fig. 5 (a) Powder XRD patterns of Na_4Si_4 samples synthesized during various reaction times at 395 °C with a 15 mL min^{-1} Ar flow. Red lines account for Na_4Si_4 reference. Si, Na, and NaOH impurities are marked on the most informative peaks. An enlarged view of the XRD pattern in the range of 26–32° is shown in (b).

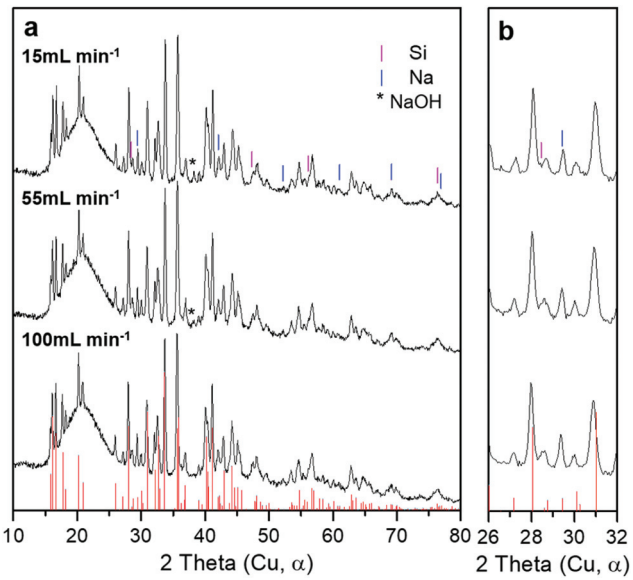

Fig. 6 (a) Powder XRD patterns of Na_4Si_4 samples synthesized with different Ar flow rates at 395 °C with a reaction time of 10 hours. Red lines account for Na_4Si_4 reference. Si, Na, and NaOH impurities are marked on the most informative peaks, where NaOH is ascribed to incidental oxidation of sample. (b) An enlarged view of the XRD pattern in the range of 26–32°.

Impact of the argon flow rate

Ma *et al.* described that a large argon flow rate (50 mL min^{-1}) resulted in excess Si, while residual Na was observed when using moderate argon flow rate (10 mL min^{-1}).[24] This sensitivity of the reaction to the gas-flow rate comes from vaporization of two products. Firstly, H_2 gas forms during the reaction (1). Secondly, reaction (1) proceeds by decomposition of NaH at *ca.* 317 °C[38] into Na, which then reacts with silicon. Nonetheless, Na is also volatile at the temperature of synthesis and can leave the reaction medium depending on the argon flow rate. Herein, the reaction was performed at 395 °C in 10 hours under different Ar flow rates (NaH : Si = 1.1 : 1) to study the impact of Ar flow on the completion of the reaction. XRD (Fig. 6) shows that the relative peak intensities for the Na impurity barely changed with the Ar flow rates and that the product Na_4Si_4 is always the major crystalline product. Therefore, the influence of Ar flow on the reaction appears negligible in the range 15–100 mL min^{-1} when using silicon nanoparticles, contrary to the bulk silicon source.[24] Hence, the higher reactivity of Si nanoparticles ensures reaction of sodium and silicon before sodium leaves the reaction medium by evaporation. The ability to perform the reaction with low dependency *versus* the Ar flow rate improves strongly the repeatability of the synthesis.

Simple approach to silicon clathrates

Silicon clathrates hold cage structures based on 4-coordinated silicon atoms. These tetrahedral frameworks can adopt a wide range of elemental substitutions to tune thermal, electrical and thermoelectric properties among others.[39,40] To assess the usefulness of the as-synthesized sodium silicide as precursor for inorganic synthesis, we have studied its thermal decomposition as a well-known pathway to type I Na_8Si_{46} and type II Na_xSi_{136} ($0 \leq x \leq 24$) silicon clathrates. Type I and type II silicon clathrates are generally obtained by thermal decomposition[7,19] or oxidation[6] of Na_4Si_4. Thermal decomposition of Na_4Si_4 under vacuum at 400–500 °C yields type I and type II clathrates,[7,19] with phase selectivity depending on various factors that are related to the vapor pressure of sodium. The impurities were the other type I/type II clathrate and *d*-Si. By using a setup to control the Na relative pressure, Krishna *et al.* reported a phase selective approach to type II clathrates.[19] By aiming for a simple and straightforward procedure, we have thermally decomposed the as-synthesized Na_4Si_4 in a very simple setup. It consists of an *h*-BN crucible introduced in a bottom-closed quartz tube heated in a vertical oven under dynamic vacuum (10^{-3} mbar).

Le Bail analysis of powder XRD patterns (Fig. 7 and Table S3) shows that the samples obtained by decomposition of Na_4Si_4 at 470 °C with a closed crucible and 440 °C with an open crucible containing Na_8Si_{46} and Na_xSi_{136} as major phases, respectively. HRTEM images of the corresponding powders are also indexed against the Na_8Si_{46} (Fig. 7c) and Na_xSi_{136} (Fig. 7d) structures, respectively, thus confirming the identity of the phases. In Fig. 7c, the amorphous oxide layer on the surface is ascribed to SiO_x or sodium silicate generated during sample manipulation.

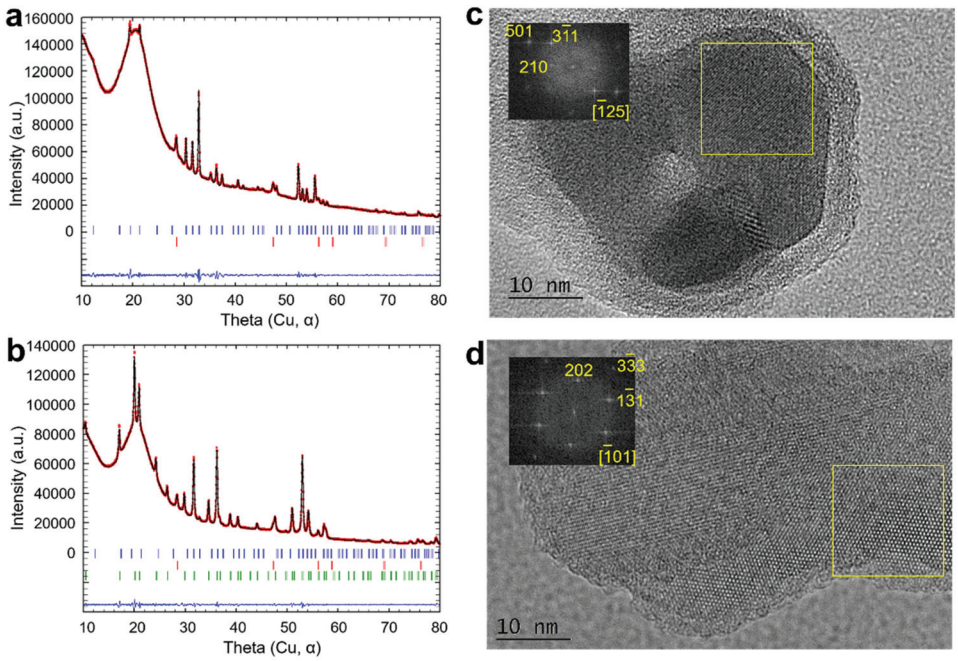

Fig. 7 (a and b) Le Bail analysis of the powder XRD patterns of products obtained by Na_4Si_4 thermal decomposition at (a) 470 and (b) 440 °C. The observed pattern, calculated pattern and difference curve are shown in red, black line and blue, respectively. Blue, green and red tick marks correspond to Na_8Si_{46} (type I), Na_xSi_{136} (type II) and Si, respectively. HRTEM images and corresponding Fast Fourier Transforms (FFTs) of powders obtained at (c) 470 °C and (d) 440 °C. FFTs are indexed along the (c) type I and (d) type II silicon clathrate structures.

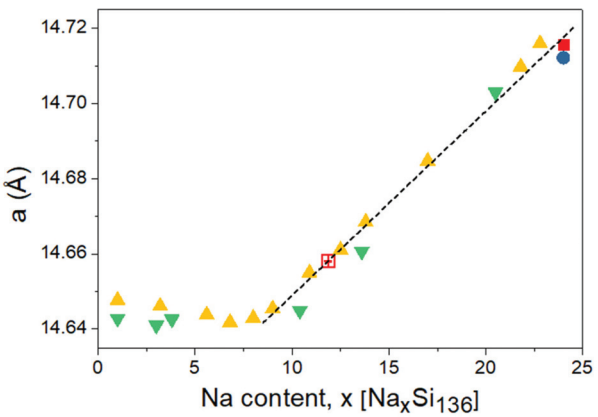

Fig. 8 *a* lattice parameter evolution with the Na content of Na_xSi_{136} ($0 \leq x \leq 24$) clathrate. Solid red square, blue circle, yellow and green triangles represent data reported by Beekman *et al.*,[42] Stefanoski *et al.*,[43] Beekman *et al.*,[44] and Reny *et al.*,[40] respectively, while the empty red square corresponds to this work. The broken line corresponds to data linear fit.

The electronic and thermal properties of Na_xSi_{136} ($0 \leq x \leq 24$) type II clathrates depend strongly on the occupancy of structural cages by Na.[40] Therefore, we have estimated the x value according to the dependency of the a cell parameter as a function of x (Fig. 8). We retrieve an overall composition of $Na_{11.86(2)}Si_{136}$ corresponding to a partial occupancy of Na sites.[7,41]

Conclusion

Herein we have shown that using silicon nanoparticles as chemical reagents provides a convenient way to solve the usual limitations of the synthesis of silicon compounds with poor thermal stability and from poorly reactive elemental silicon: the high reactivity of silicon nanoparticles enables synthesis at high yield, close to the theoretical reagent stoichiometry, and at lowered temperature below the decomposition threshold of the product, thus significantly enhancing its purity. It also enhances the robustness of the synthesis *versus* experimental conditions, especially by eliminating the dependence of the reaction *versus* gas flow. We demonstrated that the as-obtained Na_4Si_4 powder is a convenient precursor towards the selective synthesis of type I and type II silicon clathrates, thus supporting the relevance of the material for further use towards silicon-based materials.

Conflicts of interest

There are no conflicts to declare.

Acknowledgements

This work was financially supported by the China Scholarship Council, the French state funds within the framework of the Cluster of Excellence MATISSE led by Sorbonne Université, the

French Region Ile de France SESAME program and the ERC Consolidator Grant GENESIS (D. P. and I. G. R.) with Agreement Number 864850. The silicon nanoparticles were kindly provided by Nanomakers© and by ICMCB in the frame of the LabEx AMADEus (ANR-10-LABX-42) and of IdEx Bordeaux (ANR-10-IDEX-03-02).

References

1 T. Li, M. Mastro and A. Dadgar, *III–V Compound Semiconductors: Integration with Silicon-Based Microelectronics*, Taylor & Francis, 2010.
2 L. T. Canham, T. I. Cox, A. Loni and A. J. Simons, *Appl. Surf. Sci.*, 1996, **102**, 436–441.
3 R. Soref, *MRS Bull.*, 1998, **23**, 20–24.
4 F. Peng, Y. Su, Y. Zhong, C. Fan, S. T. Lee and Y. He, *Acc. Chem. Res.*, 2014, **47**, 612–623.
5 X. Chen and C. Liang, *Catal. Sci. Technol.*, 2019, **9**, 4785–4820.
6 P. Simon, Z. Tang, W. Carrillo-Cabrera, K. Chiong, B. Böhme, M. Baitinger, H. Lichte, Y. Grin and A. M. Guloy, *J. Am. Chem. Soc.*, 2011, **133**, 7596–7601.
7 H. Hiro-Omi, T. Kikudome, K. Teramura and S. Yamanaka, *J. Solid State Chem.*, 2009, **182**, 129–135.
8 O. O. Kurakevych, Y. Le Godec, W. A. Crichton, J. Guignard, T. A. Strobel, H. Zhang, H. Liu, C. Coelho Diogo, A. Polian, N. Menguy, S. J. Juhl and C. Gervais, *Inorg. Chem.*, 2016, **55**, 8943–8950.
9 S. Ganguly, N. Kazem, D. Carter and S. M. Kauzlarich, *J. Am. Chem. Soc.*, 2014, **136**, 1296–1299.
10 D. Y. Kim, S. Stefanoski, O. O. Kurakevych and T. A. Strobel, *Nat. Mater.*, 2015, **14**, 169–173.
11 R. Kumar, M. Bahri, Y. Song, F. Gonell, C. Thomas, O. Ersen, C. Sanchez, C. Laberty-Robert and D. Portehault, *Nanoscale*, 2020, **12**, 15209–15213.
12 K. Seo, K. S. K. Varadwaj, P. Mohanty, S. Lee, Y. Jo, M. H. Jung, J. Kim and B. Kim, *Nano Lett.*, 2007, **7**, 1240–1245.
13 J. G. C. Veinot, *Chem. Commun.*, 2006, 4160–4168.
14 B. M. Nolan, T. Henneberger, M. Waibel, T. F. Fässler and S. M. Kauzlarich, *Inorg. Chem.*, 2015, **54**, 396–401.
15 Y. Jiang, J. L. Carvalho-De-Souza, R. C. S. Wong, Z. Luo, D. Isheim, X. Zuo, A. W. Nicholls, I. W. Jung, J. Yue, D. J. Liu, Y. Wang, V. De Andrade, X. Xiao, L. Navrazhnykh, D. E. Weiss, X. Wu, D. N. Seidman, F. Bezanilla and B. Tian, *Nat. Mater.*, 2016, **15**, 1023–1030.
16 X. Chen, J. Guan, G. Sha, Z. Gao, C. T. Williams and C. Liang, *RSC Adv.*, 2014, **4**, 653–659.
17 X. Fan, H. Zhang, N. Du and D. Yang, *Mater. Res. Bull.*, 2012, **47**, 3797–3803.
18 M. Estruga, S. N. Girard, Q. Ding, L. Chen, X. Li and S. Jin, *Chem. Commun.*, 2014, **50**, 1454–1457.
19 L. Krishna, L. L. Baranowski, A. D. Martinez, C. A. Koh, P. C. Taylor, A. C. Tamboli and E. S. Toberer, *CrystEngComm*, 2014, **16**, 3940–3949.
20 X. Zhang, D. Neiner, S. Wang, A. Y. Louie and S. M. Kauzlarich, *Nanotechnology*, 2007, **18**, 095601.
21 M. Beekman, S. M. Kauzlarich, L. Doherty and G. S. Nolas, *Materials*, 2019, **12**, 1139.
22 T. Agrawal, R. Ajitkumar, R. Prakash and G. Nandan, *Mater. Today Proc.*, 2018, **5**, 3563–3570.
23 T. Goebel, Y. Prots and F. Haarmann, *Z. fur Krist. – New Cryst. Struct.*, 2008, **223**, 187–188.
24 X. Ma, F. Xu, T. M. Atkins, A. M. Goforth, D. Neiner, A. Navrotsky and S. M. Kauzlarich, *J. Chem. Soc., Dalton Trans.*, 2009, 10250–10255.
25 D. Mayeri, B. L. Phillips, M. P. Augustine and S. M. Kauzlarich, *Chem. Mater.*, 2001, **727**, 765–770.
26 R. Q. Cabrera, A. Salamat, O. I. Barkalov, O. Leynaud, P. Hutchins, D. Daisenberger, D. Machon, A. Sella, D. W. Lewis and P. F. McMillan, *J. Solid State Chem.*, 2009, **182**, 2535–2542.
27 M. C. Blosser and G. S. Nolas, *Mater. Lett.*, 2013, **99**, 161–163.
28 M. Shatnawi, G. Paglia, J. L. Dye, K. C. Cram, M. Lefenfeld and S. J. L. Billinge, *J. Am. Chem. Soc.*, 2007, **129**, 1386–1392.
29 J. L. Dye, K. D. Cram, S. A. Urbin, M. Y. Redko, J. E. Jackson and M. Lefenfeld, *J. Am. Chem. Soc.*, 2005, **127**, 9338–9339.
30 X. Ma, F. Xu, T. M. Atkins, A. M. Goforth, D. Neiner, A. Navrotsky and S. M. Kauzlarich, *Dalton Trans.*, 2009, 10250–10255.
31 D. Massiot, F. Fayon, M. Capron, I. King, S. Le Calvé, B. Alonso, J. O. Durand, B. Bujoli, Z. Gan and G. Hoatson, *Magn. Reson. Chem.*, 2002, **40**, 70–76.
32 L. Khouchaf, A. Hamoudi and P. Cordier, *J. Hazard. Mater.*, 2009, **168**, 1188–1191.
33 W. L. Shao, J. Shinar, B. C. Gerstein, F. Li and J. S. Lannin, *Phys. Rev. B: Condens. Matter Mater. Phys.*, 1990, **41**, 9491–9494.
34 S. Pandolfi, C. Renero-Lecuna, Y. Le Godec, B. Baptiste, N. Menguy, M. Lazzeri, C. Gervais, K. Spektor, W. A. Crichton and O. O. Kurakevych, *Nano Lett.*, 2018, **18**, 5989–5995.
35 T. R. Krawietz, D. K. Murray and J. F. Haw, *J. Phys. Chem. A*, 1998, **102**, 8779–8785.
36 J. Wang, S. Sen, P. Yu, N. D. Browning and S. M. Kauzlarich, *J. Solid State Chem.*, 2010, **183**, 2522–2527.
37 A. Courac, Y. Le Godec, C. Renero-Lecuna, H. Moutaabbid, R. Kumar, C. Coelho-Diogo, C. Gervais and D. Portehault, *Inorg. Chem.*, 2019, **58**, 10822–10828.
38 M. Kawaguchi, in International Conference on Nuclear Engineering, 2020, pp. ICONE2020-16423.
39 M. Beekman and G. S. Nolas, *J. Mater. Chem.*, 2008, **18**, 842–851.
40 E. Reny, P. Gravereau, C. Cros and M. Pouchard, *J. Mater. Chem.*, 1998, **8**, 2839–2844.

41 S. Bobev and S. C. Sevov, *J. Solid State Chem.*, 2000, **153**, 92–105.
42 M. Beekman, M. Baitinger, H. Borrmann, W. Schnelle, K. Meier, G. S. Nolas and Y. Grin, *J. Am. Chem. Soc.*, 2009, **131**, 9642–9643.
43 S. Stefanoski, M. Beekman, W. Wong-Ng, P. Zavalij and G. S. Nolas, *Chem. Mater.*, 2011, **23**, 1491–1495.
44 M. Beekman, E. N. Nenghabi, K. Biswas, C. W. Myles, M. Baitinger, Y. Grin and G. S. Nolas, *Inorg. Chem.*, 2010, **49**, 5338–5340.